

Inverting the Handedness of Circularly Polarized Luminescence from Light Emitting Polymers Using Film Thickness

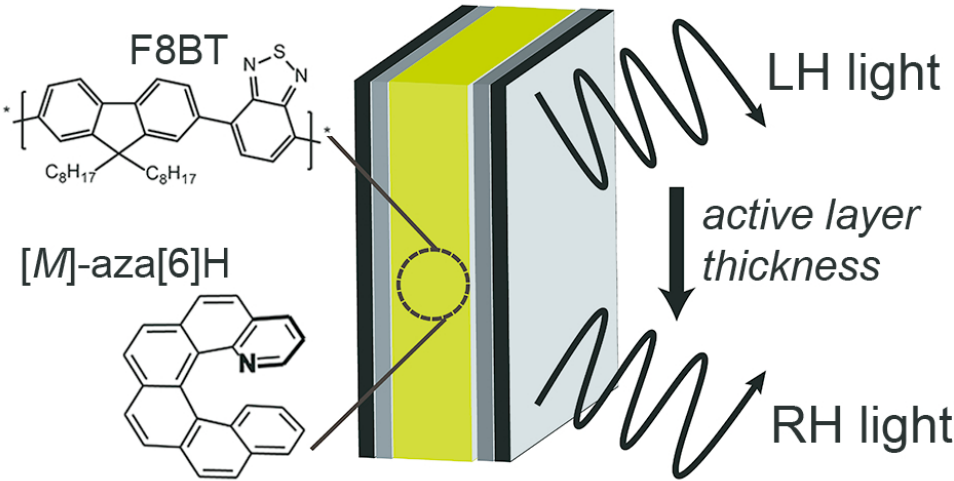
Li Wan, Jessica Wade, Francesco Salerno, Oriol Arteaga, Beth Laidlaw, Xuhua Wang, Thomas Penfold, Matthew J Fuchter, and Alasdair J. Campbell

ACS Nano, **Just Accepted Manuscript** • DOI: 10.1021/acsnano.9b02940 • Publication Date (Web): 17 Jun 2019

Downloaded from <http://pubs.acs.org> on June 19, 2019

Just Accepted

"Just Accepted" manuscripts have been peer-reviewed and accepted for publication. They are posted online prior to technical editing, formatting for publication and author proofing. The American Chemical Society provides "Just Accepted" as a service to the research community to expedite the dissemination of scientific material as soon as possible after acceptance. "Just Accepted" manuscripts appear in full in PDF format accompanied by an HTML abstract. "Just Accepted" manuscripts have been fully peer reviewed, but should not be considered the official version of record. They are citable by the Digital Object Identifier (DOI®). "Just Accepted" is an optional service offered to authors. Therefore, the "Just Accepted" Web site may not include all articles that will be published in the journal. After a manuscript is technically edited and formatted, it will be removed from the "Just Accepted" Web site and published as an ASAP article. Note that technical editing may introduce minor changes to the manuscript text and/or graphics which could affect content, and all legal disclaimers and ethical guidelines that apply to the journal pertain. ACS cannot be held responsible for errors or consequences arising from the use of information contained in these "Just Accepted" manuscripts.



ToC graphic

Inverting the Handedness of Circularly Polarized Luminescence from Light Emitting Polymers Using Film Thickness

Li Wan^{a†}, Jessica Wade^{a†}, Francesco Salerno^b, Oriol Arteaga^c, Beth Laidlaw^d, Xuhua Wang^a, Thomas Penfold^d, Matthew J. Fuchter^{b*} and Alasdair J. Campbell^{a*}

^a Department of Physics and Centre of Plastic Electronics, Imperial College London, South Kensington Campus, London SW7 2AZ, UK ^b Department of Chemistry and Molecular Sciences Research Hub, Imperial College London, White City Campus, Wood Lane, London W12 0BZ, UK ^c Departament de Física Aplicada, Universitat de Barcelona, IN2UB, Barcelona, 08028, Spain, ^d Chemistry - School of Natural and Environmental Sciences, Newcastle University, Newcastle upon Tyne, NE1 7RU, UK

ABSTRACT

The emission of circularly-polarized light is central to many applications, including data storage, quantum computation, biosensing, environmental monitoring and display technologies. An emerging method to induce (chiral) circularly-polarized (CP) electroluminescence from the active layer of polymer light emitting diodes (polymer OLEDs; PLEDs) involves blending achiral polymers with chiral small molecule additives, where the handedness/sign of the CP light is controlled by the absolute stereochemistry of the small molecule. Through the in-depth study of

such a system we report an interesting chiroptical property: the ability to tune the sign of CP light as function of active layer thickness for a fixed enantiomer of the chiral additive. We demonstrate that it is possible to achieve both efficient (4.0 cd/A) and bright (8000 cd/m²) CP-PLEDs, with high dissymmetry of emission of both left handed (LH) and right handed (RH) light, depending on thickness (thin films, 110 nm: $g_{EL} = 0.51$, thick films, 160 nm: $g_{EL} = -1.05$, with the terms “thick” and “thin” representing the upper and lower limits of the thickness regime studied), for the same additive enantiomer. We propose that this arises due to an interplay between localized CP emission originating from molecular chirality and CP light amplification or inversion through a chiral medium. We link morphological, spectroscopic, and electronic characterization in thin films and devices with theoretical studies in an effort to determine the factors that underpin these observations. Through the control of active layer thickness and device architecture, this study provides insights into the mechanisms that result in CP luminescence from CP-PLEDs, opportunities in CP photonic device design, and demonstrate high performance CP-PLEDs.

KEYWORDS *circular polarization; oleds; light emission; chiral; circular dichroism; chiroptical; thin films*

The control of dissymmetry of circularly polarized light could transform modern day electronics. For displays, direct emission of circularly polarized (CP) light in state-of-the-art organic light emitting diodes (OLEDs) could improve device efficiency and double lifetime.^{1,2} Beyond display technologies, chiral functional materials could revolutionize optical data storage, spintronic devices, as well as transforming the capabilities of environmental, pharmaceutical and biological sensors.³⁻⁹

A consensus is emerging with respect to mechanisms that underpin the direct generation of circularly polarized emission in CP-OLEDs:

1) Intrinsic CP emission from a chiral chromophore, where CP emission is defined by the following equation:¹⁰⁻¹²

$$g = \frac{4m\mu \cos \theta}{m^2 + \mu^2} \quad (\text{Eq. 1})$$

m is the magnetic transition dipole of the chromophore, μ is electric transition dipole of the chromophore, and θ is the angle between them.

2) Extrinsic CP emission through a chiral medium, such as a chiral nematic liquid crystal.⁶

To understand and improve CP emission in PLEDs, it is critical to understand the interplay between localized, conformationally induced CP emission from individual (or coupled nearest-neighbor) polymer backbones, and the effect of light propagation through a chiral medium. Experimentally, the perceived level of circular polarization can be quantified by the dissymmetry or g -factor, which in turn is calculated from the emission intensity of left-handed (LH) *versus* right-handed (RH) circularly polarized light:¹³

$$g=2\times\frac{I_L-I_R}{I_L+I_R} \quad (\text{Eq. 2})$$

Where I can be either the intensity of photoluminescence (PL) or electroluminescence (EL), and L/R refer to LH and RH emission.

It is increasingly assumed that a chiral medium based on a cholesteric stack (extrinsic CP emission through a birefringent medium) dominates the majority of CP-emissive polymer thin film devices, whether derived from a chiral small molecule – achiral polymer blend or a light-emitting polymer (LEP) with chiral side chains.^{14–16} Our previous work demonstrated CP emission from poly(9,9-dioctylfluorene-alt-benzothiadiazole) (F8BT, Figure 1a) when blended with an enantiopure chiral small additive; specifically 7 % aza[6]helicene (aza[6]H, Figure 1a) ($|g_{EL}| = 0.27$ and $|g_{PL}| = 0.5$).¹ A similar result was recently reported by Lee *et al.*, who used the same LEP (F8BT) and a commercially available chiral additive (R5011) together with an additional alignment layer.¹⁷ The alignment layer ensures the emission of linearly polarized light, which passes through a proposed cholesteric stack with high linear birefringence, to achieve very high dissymmetry in emission ($|g_{EL}| = 1.13$ and $|g_{PL}| = 0.72$).¹⁷ For the same polymer – small molecule system, by moving the recombination zone closer to the cathode within the OLED device, Jung *et al.* were able to ensure that the emitted light travels through the entire chiral medium, which increases the dissymmetry measured at the anode from $|g_{EL}| = 0.6$ to 0.8.¹⁴ Such an approach of moving the recombination zone was motivated from alternative CP-OLED studies using intrinsically chiral lanthanide emitters.^{4,18} Comparably high dissymmetry has proved harder to achieve through the use of chiral LEPs. Di Nuzzo *et al.* achieved steady-state $|g_{EL}| = 0.6$ using chiral F8BT (c-PFBT) at a high driving voltage and pulsed $|g_{EL}| = 0.8$ in thick, annealed active layers.¹⁶ In part owing to the thick active layers (> 200 nm) and requirement for high temperature annealing, which increases

1
2
3 crystallinity and reduces OLED efficiency, both studies from Lee *et al.* and Di Nuzzo *et al.* resulted
4
5 in poor device performance (F8BT + R5011: $< 200 \text{ cd/m}^2$ at 10 V and c-PFBT: $< 200 \text{ cd/m}^2$ at
6
7 25V).^{16,17} In both cases the highly dissymmetric CP EL is proposed to arise from extrinsic CP
8
9 emission, where the handedness of the light is determined by the handedness of the helical
10
11 arrangement in a proposed cholesteric stack. This is controlled by the handedness of the chiral
12
13 LEP or chiral small molecule additive.^{16,17}
14
15
16
17

18 Here we demonstrate that the combination of a chiral small molecule of a fixed handedness (single
19
20 absolute stereochemistry) and an achiral polymer can emit both LH and RH CP light, depending
21
22 on the active layer thickness. Furthermore, we achieve extraordinarily high dissymmetry factors
23
24 ($g_{\text{EL,RH}} = -1.05$ and $g_{\text{EL,LH}} = +1.10$) and state of the art device performance (4.0 cd/A with a
25
26 brightness of 2054 cd/m^2 at 10 V; it was possible to achieve a maximum brightness $> 8000 \text{ cd/m}^2$),
27
28 without the need for an alignment layer; outperforming all prior studies (Table S1). We propose
29
30 that emission from thin active layers ($< 120 \text{ nm}$ thick) is dominated by effects from *intrinsic* CP
31
32 emission, whereas when the films are thick enough ($> 120 \text{ nm}$), the dissymmetry of the emitted
33
34 light is inverted as it interacts with the chiral medium. We believe this permits the development of
35
36 highly efficient (both in terms of device performance and CP response) CP-OLED devices -
37
38 performance that is acceptable for real-world display applications, but also protocols to control the
39
40 sign of the CP light *via* simple processing of a blend material with a fixed sense of chirality.
41
42
43
44
45
46
47
48
49
50
51
52
53
54
55
56
57
58
59
60

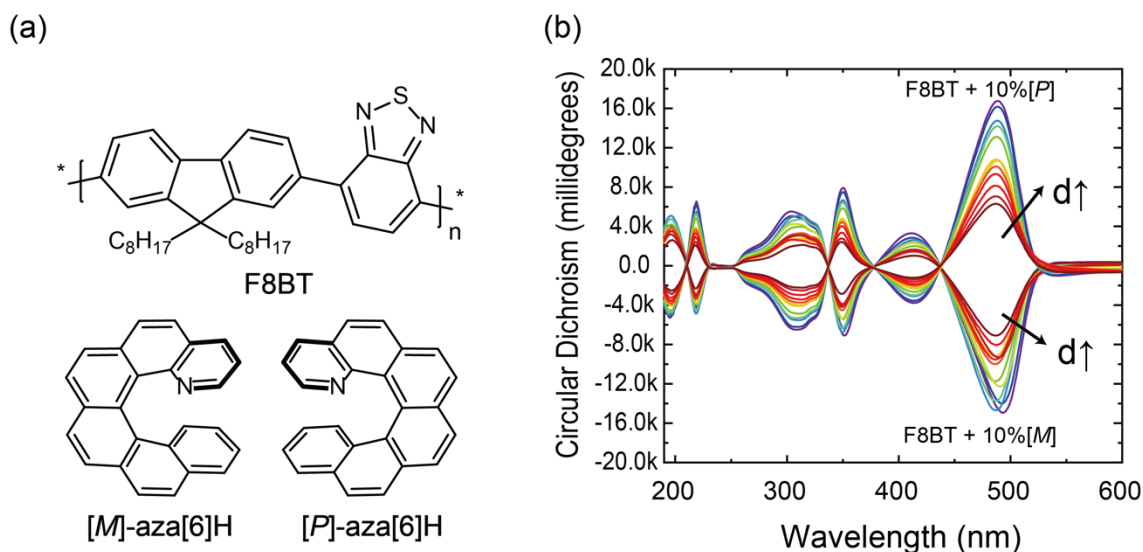


Figure 1. (a) Molecular structure of F8BT and [M]/[P] -aza[6]H. (b) Circular dichroism spectra of 10% [M]/[P] H blended F8BT films with increasing thickness d.

RESULTS AND DISCUSSION

Given the promise of the F8BT:aza[6]H blends reported in our earlier preliminary study, we chose to further study the opportunities that this material could present. Our previous studies indicated that blending a small amount (7 %) of single handedness aza[6]H with F8BT can result in strong circular dichroism (CD, > 2,000 millidegrees), CP EL and CP PL from the polymer. The naming convention for left- and right-handed light is illustrated in Figure S1. We first compared the UV-Visible absorption (UV-Vis) spectra for the neat and blended 10 % aza[6]H films, before (as-cast) and after thermal annealing (Figure S2). F8BT is a donor-acceptor copolymer, where the high-energy $\pi - \pi^*$ electronic transition ($\lambda = 330$ nm) is delocalized along the conjugated backbone.^{19,20} The lowest unoccupied molecular orbital (LUMO) is localized on the strongly accepting BT unit, and the S_1 (HOMO – LUMO) transition ($\lambda = 490$ nm) is a charge transfer state between the F8 and BT units (Figure S3a).²⁰ Blending F8BT ($M_w = 31$ K) with [P] (RH) aza[6]H results in an increase

in absorption of the high-energy transitions relative to the lower energy charge-transfer-like absorption band. There is no evidence of circular dichroism in the neat F8BT films, before or after thermal annealing (Figure S2). In the case of the F8BT:10% aza[6]H blends, as-cast films show weak CD (~ 50 millidegrees, 475 nm) that is characteristic of neat aza[6]H (Figure S2). After annealing the low-energy absorption band ($\lambda = 490$ nm) becomes broader and there is a red-shift of the absorption onset, indicating a larger distribution of conformational states. This is accompanied by a further increase in the high-energy absorption ($\lambda = 330$ nm) relative to the low-energy band (Figure S2). The annealed F8BT – [P]-aza[6]H films (110 nm thick) show a significant CD (3,000 millidegrees, $g_{\text{abs}} = +0.86$) in the polymer low-energy ($\lambda = 490$ nm) absorption band, with weaker CD (~ 1200 , 700 millidegrees, $g_{\text{abs}} = +0.40, 0.17$) in the higher-energy ($\lambda = 330$ nm, 209 nm) transitions (Figure S2). Inspired by the work of Di Bari *et al.*, appropriate controls were taken to ensure there were no artefacts present in the CD spectrum by measuring the films at different orientations with respect to the optical axis. The CD spectra of thick and thin films show no change after rotation or flipping, the combination of which rules out strong linear dichroism-linear birefringence (LD-LB) effects in the measured output (Figure S2).²¹ We note that the CPL that results from the propagation of linearly polarized light through an LD-LB chiral system is the proposed mechanism that underpins several CP-OLED studies.^{14–16} The lowest (S_1) transition demonstrates a significantly higher absorption dissymmetry than the delocalized $\pi - \pi^*$ transition (Figure S2), which could imply that there is increased torsion between the F8 and BT units, reducing the spatial overlap and decreasing angle between the electronic and magnetic dipoles (Equation 1). Our simulations show that the magnitude of both the electric and magnetic dipole moments decrease with increasing torsion angle, as the transitions become more charge-transfer in character as the angle between adjacent F8 and BT units approaches

orthogonality (Figure S3). Despite this, an increased inter-unit torsion results in a stronger luminescence dissymmetry (g_{lum}), whose sign is dependent on the direction of the torsion (Figure S3).

To better understand the impact of annealing on the conformation of the F8BT polymer backbone, we conducted Raman spectroscopy. Changes in vibrational mode intensities of F8BT due to polymer packing structures are described elsewhere.^{20,22} The F8BT inter-unit torsion can be examined by monitoring the relative intensity of the 1545 cm^{-1} and 1608 cm^{-1} Raman modes (I_{1545}/I_{1608}), which correspond to ring stretches of the BT and F8 units (see Figure S4). The optimized inter-unit torsion is 38° and I_{1545}/I_{1608} increases as the chain becomes more planar (and vice versa). As the Raman spectrum of the F8BT:aza[6]H blend ($\lambda_{\text{ex}} = 633 \text{ nm}$) also contains the vibrational signature of aza[6]H (1360 cm^{-1}), we are able to monitor both the F8BT conformation and the presence of aza[6]H simultaneously. There are very slight differences between the Raman spectra of the neat F8BT film and F8BT:aza[6]H as-cast films; indicating very small conformational changes when the chiral additive is present. After annealing, both the relative intensity of the BT (I_{1545}/I_{1608}) and aza[6]H mode (I_{1360}/I_{1608}) decrease relative to the F8 mode. This implies an increased twisting with the F8BT chains and possible phase separation of the aza[6]H from the F8BT. Further details of the Raman study are provided in the SI (see Figure S5), including measurements taken *in situ* during heating and cooling.

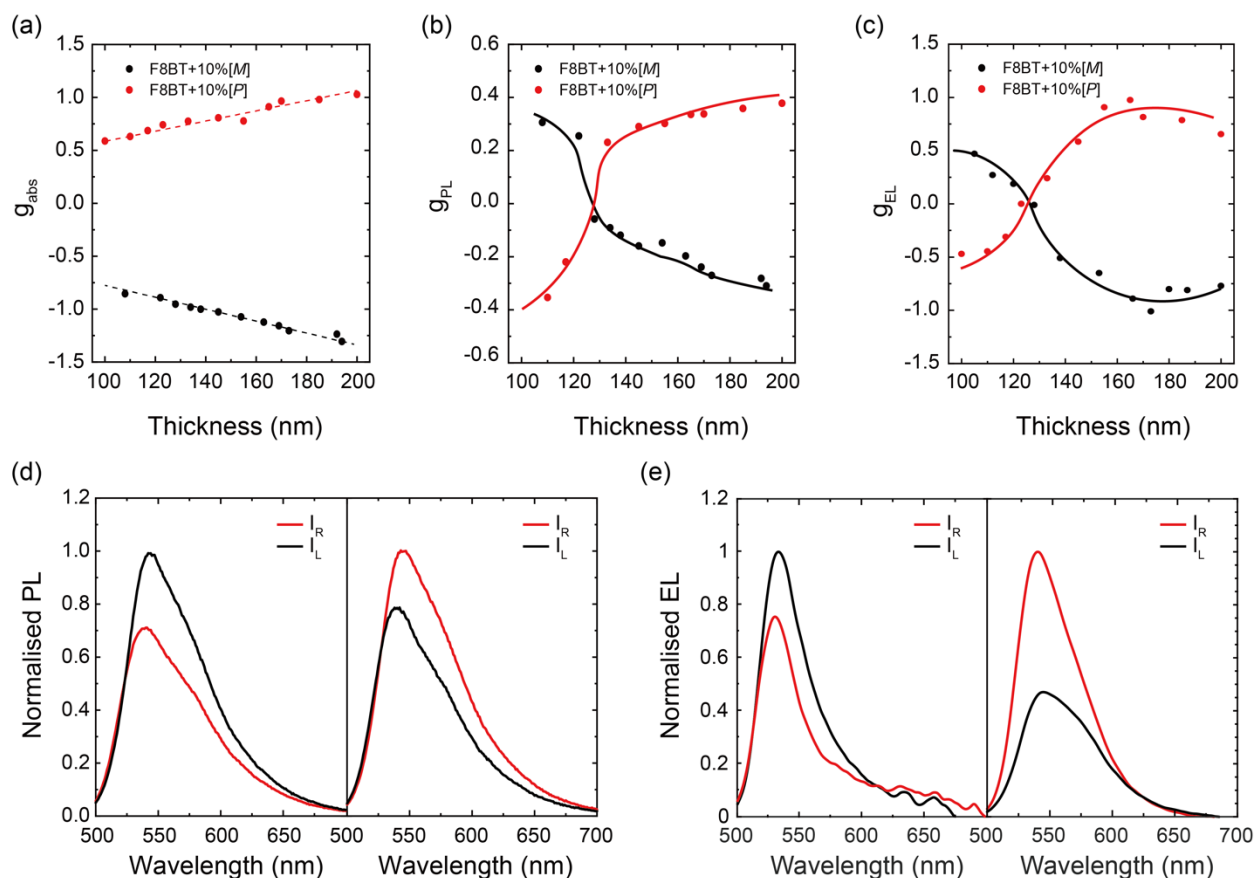


Figure 2. (a) g_{abs} as a function of film thickness, extracted from circular dichroism at $\lambda = 490$ nm. (b) g_{PL} as a function of film thickness, extracted from the emission band maximum ($\lambda = 546$ nm). (c) g_{EL} as a function of active layer thickness, extracted from the emission band maximum. (d) CPPL of 110 nm (Left) and 160 nm (Right) [M]-aza[6]H blended films. (e) CPEL of [M]-aza[6]H blended devices with 110 nm (Left) and 160 nm (Right) active layers. Device Structure: ITO/PEDOT:PSS/TFB/F8BT+10% [M]/[P]-aza[6]H/Ca/Al.

Following the identification of annealing conditions that lead to a large induced CD, we examined the impact of film thickness on the dissymmetry of absorption and emission. Spin-coating was used to obtain film thicknesses between 100 and 200 nm, chosen to be optimum for display technologies. In general, the width of the low energy absorption band ($\lambda = 490$ nm) slightly

increases with increasing film thickness, indicating a broader distribution of polymer chain conformations in the thicker films, but the position of the absorption maximum does not change (Figure S6). The absorption shows increasing induced CD with increasing film thickness (Figure 1b), with a linear increase of g_{abs} as a function of film thickness (Figure 2a). At the same time, the photoluminescence spectra become broader, with thicker films giving slightly red-shifted PL ($\lambda_{\text{thick}} = 547 \text{ nm}$, $\lambda_{\text{thin}} = 540 \text{ nm}$) and a longer low-energy tail (Figure S6), which could be due to scattering and reflection in the thicker films with multiple polymer backbone orientations. The extracted dissymmetry factors (Figure 2) indicate that whilst g_{abs} increases gradually in the thickness range considered (100 – 200 nm), the g_{PL} first decreases (100 – 110 nm) to zero, and then inverts sign (> 120 nm) entirely. Using the mirror image enantiomer of the chiral small molecule – [M] (LH) aza[6]-H – gives an equal but opposite response: g_{PL} varies from + 0.35 (100 nm) to – 0.35 (200nm). It is interesting to note that the surface morphology of the F8BT:aza[6]-H blends show little change before and after annealing (Figure S7). CP-PLEDs with same thickness range for the active layer were fabricated (see Methods section for fabrication details) with the device architecture shown in Figure S8. The extracted g_{EL} showed the same trend as the g_{PL} , for the [M]-aza[6]-H blends, g_{EL} varies from + 0.50 (100 nm) to – 1.00 (200nm), and the response inverts for [P]-aza[6]-H blends. Above certain thicknesses, the g_{EL} is negative (*i.e.* RH emission) for F8BT:[M]-aza[6]-H blends, which is consistent with the sign of CP light observed in our prior study.¹ If the active layer is less than 120 nm, the handedness of CPEL fully inverts however. If the active layer is between 120 nm and 185 nm thick (Figure S9), the shape of the EL does not change and the blend has an emission maximum of $\sim 540 \text{ nm}$. The EL shape changes if the thickness increases (micro-cavity effects) or decreases (interfacial effects between active layer and cathode) beyond this range (Figure S9).^{23,24} We note that OLED outcoupling not only changes the

shape of the EL spectrum, but also the intensity due to the position and orientation of the emissive molecules (outcoupling is strongest towards the center of the device, and also with dipoles aligned in-plane); both will contribute to the apparent g_{EL} . For $[M]$ -aza[6]H blend devices, in the thick device regime (140 nm), we can achieve an extraordinarily high dissymmetry value ($g_{EL} = -1.05$).

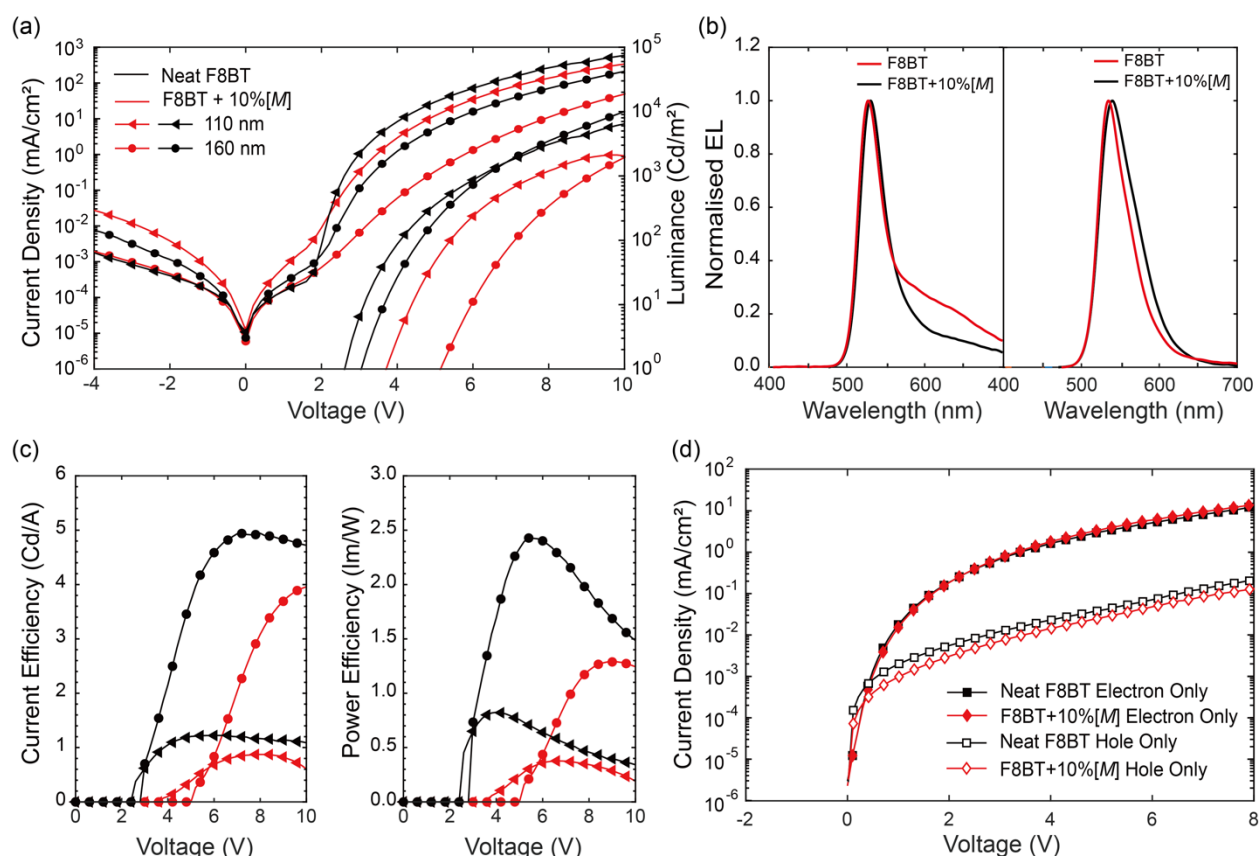


Figure 3. (a) Current-Voltage-Luminance curves of neat F8BT reference devices (black) and $[M]$ -aza[6]H blended devices (red) with thickness of 110 nm (triangles) and 160 nm (circles). (b) Normalised EL spectra of reference devices and $[M]$ -aza[6]H blended devices. (c) Current efficiency and power efficiency of the reference devices and $[M]$ -aza[6]H blended devices. (d) Single carrier Current-Voltage curves. Device structures: (a)-(c) ITO/PEDOT:PSS/TFB/F8BT+10% $[M]$ -aza[6]H/Ca/Al; (d) Hole only:

ITO/PEDOT:PSS/TFB/F8BT+10%[M]-aza[6]H/MoO₃/Au (Hole injection from ITO); Electron only: ITO/ZnO/F8BT+10%[M]-aza[6]H/Ca/Al (Electron injection from Al)

In terms of device performance, current-voltage-luminance (JVL) curves all show an increase in the current density at ~ 2.3 V, which is approximately the built-in potential (V_{bi}) in our device structure (Figure S7). We compare devices with active layer (F8BT:[M]-aza[6]H) thicknesses of 110 nm and 160 nm, as these show minimal changes in the shape of the EL spectra compared to neat F8BT (Figure 3b). We achieve the best known performance for CP-OLEDs (Table S1) in both 110 nm devices (RH CP emission) and 160 nm devices (LH CP emission) (Figure 3a, Table S2), with current efficiencies of 4.0 cd/A (160 nm) and 0.9 cd/A (110 nm) and luminance > 2000 cd/m² (@ 10 V, Figure 3c).^{1,16,17,25} Given that one of the proposed uses of a CP-OLED is within AMOLED displays, which typically combine a quarter wave plate (QWP) with a linear polarizer (LP) to act as an anti-glare filter,² we sought to examine how this display context could allow for a clear comparison between our CP-OLEDs and a comparable non-CP device (Figure S10). As light emission in neat F8BT devices is randomly polarized, the current efficiency decreases by 50% when a QWP and LP are placed in the path of light emission, from 4.9 cd/A to 2.2 cd/A for 160 nm films (Table S2). However, due to the high dissymmetry of emission in the F8BT:aza[6]H devices considered here, the current efficiency only decreases by 25%, from 4.0 cd/A to 3.0 cd/A: giving a comparable performance with a non-blended active layer within the context of a display (Table S2). To identify any impact of the chiral additive on charge injection and transport in F8BT, we fabricated hole only and electrons only diodes (Figure 3d). The electron current is unchanged by the addition of the chiral additive, while the hole current is only slightly reduced. This confirms that this chiral additive causes little change in current flow, and hence injection, transport and trapping, within the LEP. We have investigated the impact of electric field strength on g_{EL} by

measuring CPEL at varying applied voltage for both thick (160 nm) and thin (110 nm) films. As can be seen in Figure S11, g_{EL} is constant as a function of internal electric field as the bias is increased, implying that the inversion of g_{EL} reported here is not due to the electric field strength alone.

Given the role of cathode reflectivity on the magnitude of g_{EL} in prior studies, we have investigated this effect within our devices.¹⁴ The reflectivity of the metal cathode (Figure S12-S16) was modified by controlling the thickness of the calcium, and increases the RH emission for both thick and thin films, resulting in opposite changes in the apparent dissymmetry (g_{EL}). For the F8BT:[M]aza[6]H blends, increasing the thickness of the calcium results in an increase of RH g_{EL} from -0.51 to -0.80 for the 140 nm (thick) film, while for the 110nm (thin) film it results in a decrease in the magnitude of the LH g_{EL} from +0.50 to +0.39 (Figure S14). The impact of aluminium thickness was also considered, but as 25 nm Ca already has a high reflectivity, the effect of aluminium thickness on g_{EL} was less obvious (Figure S12- S16).

To the best of our knowledge, inversion of CP emission in CP-PLEDs for a fixed handedness of chiral material (single absolute stereochemistry) has rarely been observed and has not been discussed or studied in detail (Table S3).¹² In 2003, Meskers *et al.* observed a sign change in the CD of chiral polyfluorene films as a function of film thickness, which they attributed to poor film uniformity and low coverage.²⁶ They showed that PFO thin films with non-perpendicular electric and magnetic transition dipoles give one sign of CD, whereas selective reflection of cholesteric stacks gives the opposite.²⁷ This framework of understanding does not fit the inversion of CP-EL handedness that we observe here. Chen *et al.* synthesized a chiral oligofluorene F(5*S*)7F-(10*S*)2, and measured opposite g_{PL} between pristine and annealed films.²⁸ They predicted that this is due to differences in chirality between single molecules and bulk packing, but did not investigate the

effect in detail. The most similar prior work is that of Lee *et al.*, using F8BT and R5011, whose results indicated that when the recombination zone is moved from the cathode to the anode, the handedness varies from negative to positive.¹⁵ Unfortunately this finding was not addressed in their discussion.^{15,17}

Our understanding of the mechanism that underpins our data is as follows: a uniform, disordered blend film of F8BT:aza[6]H forms after spin-coating (Figure S2), with no evidence of CD, CP PL or CP EL. The films are annealed above the F8BT glass transition temperature (140 °C), which permits the F8BT chains to become more flexible and the aza[6]H more mobile within the blend (Figure S4). The F8BT chains become twisted with a preferential handedness (which depends on the chiral aza[6]H), which results in non-orthogonal electric and magnetic transition dipole moments for the F8 to BT charge transfer transition (S_1), as shown in Figure S3. The layers of twisted F8BT subsequently form a chiral medium whose handedness depends on the chiral additive and/or polymer twist and can be related to the sign of the Cotton effect at 490 nm in the CD spectrum (Figure 2). The linearly increasing g_{abs} and transmission Mueller Matrix data (Figure S17) we measure imply that the magneto-electronic coupling terms do not change and are consistent with the formation of chiral structures within the films.

Taken together, our data implies extrinsic linear effects (LD-LB) are not responsible for CP emission in the films and devices here, in contrast to the mechanisms proposed in prior studies.^{14-16,21} Specifically, the absence of an alignment layer, negligible LD or LB in the Mueller Matrix (Figure S17), lack of sign change in CD spectra acquired from the flipped samples or any feature in cross-polarized microscope images (Figure S2), and similar handedness emission in PL and EL measurements (which consider different sides of the film) all discount linear effects (LD-LB). On

the other hand, consistent with previous work, no measurable CP Bragg reflectance is observed, and the pitch length required to produce chiroptical effects of these magnitudes *via* reflection ($\sim 0.5 - 1.5 \mu\text{m}$) far exceeds the film thicknesses considered here.^{16,29} We propose instead that the apparent dissymmetry of emitted light, as a function of thickness, is due to the interplay of two distinct mechanisms at the different thickness regimes; localized CP emission originating from molecular chirality (for example from twisted polymer chains, coupling of adjacent polymer chains, or nano-scale chiral aggregates) and CP light amplification or inversion *via* propagation through a chiral medium.³⁰

The fundamental phenomena that underpin the chiral medium effects remain to be fully elucidated, but one potential mechanism may be circular scattering from the multi-domain disordered cholesteric phase, as proposed for F8BT with chiral side chains (c-PFBT).¹⁶ Di Nuzzo *et al.* predict that g_{EL} should increase as the recombination zone moves deeper into the device, as well as a specific variation with wavelength depending on the active layer optical constants. These predictions can be observed in this study – as the active layer gets thicker, the recombination zone moves deeper into the device, which could result in a switch in the dominant emission from molecular (thin films) to cholesteric multi-domain scattering (thick films). The variation of g_{EL} with wavelength for the device thickness considered here demonstrate the predicted peak followed by a roll-off to longer wavelengths (Figure S18) (although we note though that this is not true for all device thicknesses, and that these measurements are particularly sensitive to the choice of quarter wave plate). In addition, the circular birefringence from the chiral medium which show a similar wavelength dependence in the emission region (Figure S17) may contribute to the variation in g_{EL} due to the established inverse-square relationship between outcoupled light intensity and refractive index which occurs in organic LEDs.

CONCLUSIONS

In summary, through the combination of an achiral polymer and chiral small molecule additive we have observed an interesting chiroptical phenomenon, where the apparent dissymmetry of CP EL and CP PL can be tuned through the thickness of the active layer alone. We can achieve extraordinarily high g-factors for both left and right handed CPL through the use of a single handed (enantiopure) aza[6]H additive, without the need for an alignment layer. Additionally, the device performance shows a marked improvement on previous publications, where either device performance or g_{EL} could be improved, but not both. The mechanisms disclosed here provide insight into chiral emission within CP-OLEDs and provides opportunities to study and utilize intrinsic CPL within a chiral additive – achiral LEP system. We believe that this will have a significant impact on the improvement of CP-OLED performance and other studies of chiral materials in CPL research: it is no longer necessary to assume all high dissymmetry CP-emission in CP-PLED originates from the propagation of light through a thick chiral medium, but can be achieved through the interplay of other effects. This will provide a set of design rules for LEPs and chiral additives and establishes the benefits of these active layers in other CP-sensitive technologies.

EXPERIMENTAL

Aza[6]helicene was prepared as previously reported and separated using preparative chiral HPLC.^{1,31}

Solution Preparation and thin film deposition: F8BT and aza[6]helicene were dissolved in toluene to a concentration of 35 mg/mL and blended to form a 10% aza[6]H solution. Thin films of various thickness were controlled by changing the spin-speed (1200 rpm – 5000 rpm) and deposited on clean fused silica substrates. The cleaning process for all substrates involved rinsing in an ultrasonic bath with acetone, isopropyl alcohol (IPA) and Hellmanex III (Sigma Aldrich) and deionized water for 30 minutes. These were transferred to a plasma asher for 3 minutes at 80 W before spin-coating. All annealed samples were annealed for 10 min in a nitrogen atmosphere (glovebox, < 0.1 ppm H₂O, < 0.1 ppm O₂) in the dark. Film thicknesses of all films were measured using a Dektak 150 surface profiler.

Photophysical and Morphological Characterization: Absorption and PL spectra of the thin films were measured by a Cary 300 UV–Vis spectrometer (Agilent Technologies) and a FLS 1000 (Edinburgh Instruments). PL measurements were made at a 45° incident angle using a 475 nm excitation wavelength. Mueller Matrix Spectroscopic Ellipsometry was performed using a Woollam VASE in transmittance mode. *In situ* Raman spectroscopy was performed using a Renishaw inVia Raman Microscope which was calibrated using the Silicon Raman band at 520.5 cm⁻¹. The laser spot size was 1 μm² and the excitation wavelength was 633 nm for a 20-second accumulation time.

Circular Dichroism, CPEL/CPPL: Circular Dichroism measurements were performed using a Chirascan (Applied Photophysics) spectrophotometer. Left-handed and right-handed CP emission spectra were collected using a combination of linear polarizer and zero-order quarter-wave plate (546 nm, Thorlabs) placed before the photodetector. The background introduced by the polarizer, the quarter-wave plate and the silica substrates were corrected by using the CP-PL results from a

blank sample. The dissymmetry factor g in the CP-PL spectra was calculated from the equation $g = 2(I_L - I_R)/(I_L + I_R)$, $|g| \leq 2$. Here, I_L and I_R are the left-handed and right-handed emission intensities. A similar method was used to analyze the CP-EL spectra. EL spectra from the PLED were recorded using an Ocean Optics USB 2000 charge-coupled spectrophotometer. All CPEL measurements are carried out after measuring with only linear polarizer to ensure negligible linear polarization or random polarization, which should be considered in all CP emission measurements. The thickness dependent CPEL measurements are carried out under constant current (1 mA).

OLED Fabrication and characterization: Pre-patterned ITO substrates (Thin Film Devices, 20 ohms/sq, 1450 Å) were cleaned as described above for the silica substrates before the deposition of poly(3,4-ethylenedioxythiophene):poly(styrenesulfonate) (PEDOT:PSS) (H.C. Starck GmbH) (55 nm). Active layer deposition was the same as for the thin film studies, followed by the thermal evaporation of a 25 nm Ca layer, capped by with 100 nm Al layer onto the organic layer under vacuum level of 1×10^{-7} mbar. J-V-L characterization (pixel area = 0.045 cm²) was performed using a Keithley 2400 and Konica Minolta LS-110 Luminance Meter. PLED emission was assumed to be Lambertian. EL spectra were measured using an Ocean Optics USB 2000 charge-coupled device spectrophotometer. The display efficiency and luminance were carried out with the geometry of Device-QWP-LP-Candela meter to perform a similar geometry in state-of-the-art display design.

ASSOCIATED CONTENT

Supporting Information

The Supporting Information is available free of charge on the ACS Publications website. The Supporting Information includes detailed steady-state and *in situ* spectroscopy, molecular modelling and device data.

AUTHOR INFORMATION

Corresponding Author

* *Matthew J. Fuchter*, m.fuchter@imperial.ac.uk

* *Alasdair J. Campbell*, alasdair.campbell@imperial.ac.uk

Author Contributions

All authors have given approval to the final version of the manuscript. ‡These authors contributed equally.

ACKNOWLEDGMENTS

We would like to acknowledge the Engineering and Physical Science Research Council for funding this work (EP/P000525/1, EP/L016702/1, EP/R00188X/1, EP/R021503/1). The authors would also like to thank Matthew Roberts and Cambridge Display Technology Limited (Company number 02672530) for providing the polymers and for their contributions to our understanding of the system. We are grateful to Professor Ji-Seon Kim at Imperial College London for providing access to the Raman spectrometer and Applied Photophysics for their advice on Circular Dichroism measurements.

References

- (1) Yang, Y.; Da Costa, R. C.; Smilgies, D. M.; Campbell, A. J.; Fuchter, M. J. Induction of Circularly Polarized Electroluminescence from an Achiral Light-Emitting Polymer *via* a Chiral Small-Molecule Dopant. *Adv. Mater.* **2013**, *25*, 2624–2628.
- (2) Brandt, J. R.; Wang, X.; Yang, Y.; Campbell, A. J.; Fuchter, M. J. Circularly Polarized Phosphorescent Electroluminescence with a High Dissymmetry Factor from PHOLEDs Based on a Platinahelicene. *J. Am. Chem. Soc.* **2016**, *138*, 9743–9746.
- (3) Zinna, F.; Giovanella, U.; Bari, L. Di. Highly Circularly Polarized Electroluminescence from a Chiral Europium Complex. *Adv. Mater.* **2015**, *27*, 1791–1795.
- (4) Zinna, F.; Pasini, M.; Galeotti, F.; Botta, C.; Di Bari, L.; Giovanella, U. Design of Lanthanide-Based OLEDs with Remarkable Circularly Polarized Electroluminescence. *Adv. Funct. Mater.* **2017**, *27*, 1603719.
- (5) Dor, O. Ben; Yochelis, S.; Mathew, S. P.; Naaman, R.; Paltiel, Y. A Chiral-Based Magnetic Memory Device without a Permanent Magnet. *Nat. Commun.* **2013**, *4*, 2256.
- (6) Manoli, K.; Magliulo, M.; Torsi, L. Chiral Sensor Devices for Differentiation of Enantiomers. *Top. Curr. Chem.* **2013**, *341*, 133–176.
- (7) Huang, H.; Bian, G.; Zong, H.; Wang, Y.; Yang, S.; Yue, H.; Song, L.; Fan, H. Chiral Sensor for Enantiodiscrimination of Varied Acids. *Org. Lett.* **2016**, *18*, 2524–2527.
- (8) Maia, A. S.; Ribeiro, A. R.; Castro, P. M. L.; Tiritan, M. E. Chiral Analysis of Pesticides and Drugs of Environmental Concern: Biodegradation and Enantiomeric Fraction. *Symmetry* **2017**, *9*, 196.
- (9) Zhang, X.; Yin, J.; Yoon, J. Recent Advances in Development of Chiral Fluorescent and Colorimetric Sensors. *Chem. Rev.* **2014**, 4918–4959.
- (10) Nakai, Y.; Mori, T.; Inoue, Y. Theoretical and Experimental Studies on Circular Dichroism of Carbo[N]Helicenes. *J. Phys. Chem. A* **2012**, *116*, 7372–7385.

- (11) Blok, P. M. L.; Dekkers, H. P. J. M. Discrimination between $3\pi\pi^*$ and $3n\pi^*$ States in Organic Molecules by Circular Polarization of Phosphorescence. *Chem. Phys. Lett.* **1989**, *161*, 188–194.
- (12) Han, J.; Guo, S.; Lu, H.; Liu, S.; Zhao, Q.; Huang, W. Recent Progress on Circularly Polarized Luminescent Materials for Organic Optoelectronic Devices. *Adv. Opt. Mater.* **2018**, *6*, 1880538.
- (13) Purdie, N.; Swallows, K. A.; Murphy, L. H.; Purdie, R. B. Analytical Applications of Circular Dichroism. *J. Pharm. Biomed. Anal.* **1989**, *7*, 1519–1526.
- (14) Jung, J.; Lee, D.; Kim, J.; Yu, C. Circularly Polarized Electroluminescence by Controlling the Emission Zone in a Twisted Mesogenic Conjugate Polymer. *J. Mater. Chem. C* **2018**, *6*, 726–730.
- (15) Lee, D.-M.; Song, J.-W.; Lee, Y.-J.; Yu, C.-J.; Kim, J.-H. Control of Circularly Polarized Electroluminescence in Induced Twist Structure of Conjugate Polymer. *Adv. Mater.* **2018**, *30*, 1705692.
- (16) Di Nuzzo, D.; Kulkarni, C.; Zhao, B.; Smolinsky, E.; Tassinari, F.; Meskers, S. C. J.; Naaman, R.; Meijer, E. W.; Friend, R. H. High Circular Polarization of Electroluminescence Achieved *via* Self-Assembly of a Light-Emitting Chiral Conjugated Polymer into Multidomain Cholesteric Films. *ACS Nano* **2017**, *11*, 12713–12722.
- (17) Lee, D.-M.; Song, J.-W.; Lee, Y.-J.; Yu, C.-J.; Kim, J.-H. Control of Circularly Polarized Electroluminescence in Induced Twist Structure of Conjugate Polymer. *Adv. Mater.* **2017**, *29*, 1700907.
- (18) Zinna, F.; Di Bari, L. Emerging Field of Chiral Ln(III) Complexes for OLEDs. In *Lanthanide-Based Multifunctional Materials*; 2018; pp 171–194.
- (19) Jespersen, K. G.; Beenken, W. J. D.; Zaushitsyn, Y.; Yartsev, A.; Andersson, M.; Pullerits, T.; Sundström, V. The Electronic States of Polyfluorene Copolymers with Alternating Donor-Acceptor Units. *J. Chem. Phys.* **2004**, *121*, 12613–12617.

- (20) Donley, C. L.; Zaumseil, J.; Andreasen, J. W.; Nielsen, M. M.; Sirringhaus, H.; Friend, R. H.; Kim, J.-S. Effects of Packing Structure on the Optoelectronic and Charge Transport Properties in. *J. Am. Chem. Soc.* **2005**, *127*, 12890–12899.
- (21) Albano, G.; Salerno, F.; Portus, L.; Porzio, W.; Aronica, L. A.; Di Bari, L. Outstanding Chiroptical Features of Thin Films of Chiral Oligothiophenes. *ChemNanoMat* **2018**, *4*, 1059–1070.
- (22) Schmidtke, J. P.; Kim, J.-S.; Gierschner, J.; Silva, C.; Friend, R. H. Optical Spectroscopy of a Polyfluorene Copolymer at High Pressure: Intra- and Intermolecular Interactions. *Phys. Rev. Lett.* **2007**, *99*, 167401.
- (23) Costa Dantas Faria, J.; Campbell, A. J.; McLachlan, M. A. Fluorene Copolymer Bilayers for Emission Colour Tuning in Inverted Hybrid Light Emitting Diodes. *J. Mater. Chem. C* **2015**, *3*, 4945–4953.
- (24) Burin, A. L.; Ratner, M. A. Exciton Migration and Cathode Quenching in Organic Light Emitting Diodes. *J. Phys. Chem. A* **2000**, *104*, 4704–4710.
- (25) Brandt, J. R.; Salerno, F.; Fuchter, M. J. The Added Value of Small-Molecule Chirality in Technological Applications. **2017**, *1*, 45.
- (26) Craig, M. R.; Jonkheijm, P.; Meskers, S. C. J.; Schenning, A. P. H. J.; Meijer, E. W. The Chiroptical Properties of a Thermally Annealed Film of Chiral Substituted Polyfluorene Depend on Film Thickness. *Adv. Mater.* **2003**, *15*, 1435–1438.
- (27) Lakhwani, G.; Meskers, S. C. J. Insights from Chiral Polyfluorene on the Unification of Molecular Exciton and Cholesteric Liquid Crystal Theories for Chiroptical Phenomena. *J. Phys. Chem. A* **2012**, *116*, 1121–1128.
- (28) Geng, Y.; Trajkovska, A.; Katsis, D.; Ou, J. J.; Culligan, S. W.; Chen, S. H. Synthesis, Characterization, and Optical Properties of Monodisperse Chiral Oligofluorenes. *J. Am. Chem. Soc.* **2002**, *124*, 8337–8347.
- (29) Schulz, M.; Zablocki, J.; Abdullaeva, O. S.; Brück, S.; Balzer, F.; Lützen, A.; Arteaga, O.;

- 1
2
3 Schiek, M. Giant Intrinsic Circular Dichroism of Prolinol-Derived Squaraine Thin Films.
4 *Nat. Commun.* **2018**, *9*, 2413.
5
6
7
8 (30) Arteaga, O. Natural Optical Activity vs Circular Bragg Reflection Studied by Mueller
9 Matrix Ellipsometry. *Thin Solid Films* **2016**, *617*, 14–19.
10
11
12 (31) Yang, Y.; Rice, B.; Shi, X.; Brandt, J. R.; Correa Da Costa, R.; Hedley, G. J.; Smilgies, D.
13 M.; Frost, J. M.; Samuel, I. D. W.; Otero-De-La-Roza, A.; Johnson, E. R.; Jelfs, K. E.; Nelson,
14 J.; Campbell, A. J.; Fuchter, M. J. Emergent Properties of an Organic Semiconductor Driven
15 by Its Molecular Chirality. *ACS Nano* **2017**, *11*, 8329–8338.
16
17
18
19
20
21
22
23
24
25
26
27
28
29
30
31
32
33
34
35
36
37
38
39
40
41
42
43
44
45
46
47
48
49
50
51
52
53
54
55
56
57
58
59
60